STUDY OF MECHANICAL PROPERTIES OF 3D-PRINTED SILICONE FOR CUSHIONING APPLICATIONS

ELIJAH LIM RONG YAO

UNIVERSITI TUNKU ABDUL RAHMAN

STUDY OF MECHANICAL PROPERTIES OF 3D-PRINTED SILICONE FOR CUSHIONING APPLICATIONS

ELIJAH LIM RONG YAO

A project report submitted in partial fulfilment of the requirements for the award of Bachelor of Mechanical Engineering with Honours

Lee Kong Chian Faculty of Engineering and Science
Universiti Tunku Abdul Rahman

May 2026

DECLARATION STATEMENT

I hereby declare that this project report is my original work, with all sources duly acknowledged, and that it has not been submitted previously or concurrently for any degree or award at UTAR or elsewhere. I also declare the following *(check the boxes if applicable)*:

☐ Generative AI tools (e.g., ChatGPT, Gemini, Copilot, etc.) were used for language refinement, such as grammar correction and readability improvement.

☐ Vibe coding tools and/or frameworks (e.g., Replit Agent, Cursor Composer, Bolt, etc.) were used in project development.

☑ Other declaration(s), if any (*please consult your supervisor for guidance in completing this section*):

ChatGPT was only used to assist in sourcing academic journals and articles. No artificial intelligence tools were used in the writing of this report, summarising articles and journals.

I take full responsibility for the originality, accuracy, and integrity of all content presented in this report. No Generative AI tools were used to manipulate project data and results in ways that could cause falsification or misrepresentation.

Name	:	Elijah Lim Rong Yao
ID No.	:	2102459
Date	:	04th May 2026

COPYRIGHT STATEMENT

ACKNOWLEDGEMENTS

I would like to express my gratitude to Dr Jaslyn Low Foon Siang as my research supervisor for her advice, guidance, and patience all throughout this research project. I would also like to thank my parents, brother, and friends who helped me and encouraged me throughout this final year project until its completion. Lastly, I want to thank God for giving me the strength through all the hardships in completing this final year project.

ABSTRACT

3D-printed silicones possess many beneficial characteristics for household applications however, there is limited research into this field. Most of the research done focuses on biomedical and industrial applications despite the growing demand for ergonomic and customised products from general consumers which may be addressed through the use of 3D-printed silicones. This study focuses on the ability to use 3D-printed silicones as a replacement for conventional cushioning materials such as memory foam, rubber latex foam, and polyurethane. 4 infill patterns which include grid, gyroid, triangle, and stars were printed each with 4 different infill percentages of 40%, 50%, 60%, and 70%. All these printed samples were subjected to compression tests to obtain parameters such as the stress-strain relationship, Young's modulus, and SAG factor of each sample. It was found that all the samples had low Young's modulus, high SAG factor, and desirable stress-strain relationships. These characteristics were also compared with the amount of material used to print each pattern as the required volume of silicone needed to form each geometry is different from each other. By comparing these parameters together, it was found that all these samples had characteristics that showed potential to replace cushioning materials with the gyroid pattern exhibiting the most desirable characteristic by having the highest SAG factor with an average of 6.125 across the different infill densities; smooth stress-strain relationship; lowest material usage with an average of 4730.323mm^2; and moderate Young's. Further study into this field is highly recommended as this study shows the potential for 3D-printed silicones to be an alternative to conventional cushioning materials if the manufacturing process can be optimised.

Keywords: additive manufacturing; silicones; 3D-printing; physical properties; mechanical properties; cushion material;

Subject Area: TS155-194 Production Management. Operations Management

TABLE OF CONTENTS

LIST OF TABLES

LIST OF FIGURES

LIST OF SYMBOLS / ABBREVIATIONS

ρ	density, kg/m^3
DIW	Direct Ink Writing
FDM	Fused Deposit Modelling
SLS	Selective Laser Sintering
MJ	Material Jetting
VPP	Vat Polymerisation Printing
DLP	Digital Light Processing
PDMS	Polydimethylsiloxane
UI	User Interface
SAG factor	Support Factor

LIST OF APPENDICES

CHAPTER 1

INTRODUCTION

1.1 General Introduction

Silicone is a synthetic polymer mainly composed of polysiloxane and other elements such as hydrogen, carbon, and oxygen. It is used in all sorts of applications such as automotive grease, electrical for insulation, medicine for molds and many others. This is due to the many beneficial characteristics of silicone which include low toxicity, low thermal and electrical conductivity, hydrophobic, high durability, and thermal stability. These characteristics have allowed silicone to become a popular material in many industries.

Additive manufacturing is a modern manufacturing process that has allowed researchers and industrial players to improve products and research methods. This is due to the benefits of additive manufacturing such as ease of use, rapid prototyping, and ability to create complex internal 3D structures that are just not possible with conventional manufacturing techniques. 3D-printing as it is more commonly known, has revolutionized the manufacturing industry as large scale companies are able to incorporate large scale 3D-printers in their manufacturing processes while small companies or consumers are able to utilize small-sized 3D printers for home projects or small-scale production.

With all the benefits from silicone as a material and 3D-printing as a manufacturing process, 3D-printed silicones have great potential in household applications. Silicone has always been desirable for household applications due to its physical properties, especially for kitchen utensils, cookware and insulating electrical appliances. Examples of potential usages in household goods include toothbrushes, kitchen utensils, cookery handles, food safe containers, airtight/waterproof linings in appliances, and wearables.

With these two technologies that have immense benefits compared to conventional materials and manufacturing processes, it is obvious that industry and scientific communities would attempt to combine these technologies to further improve upon each other to innovate new products or techniques. However, combining these technologies is not as simple as it seems due to the characteristics of silicone as a material and 3D-printing techniques. Silicone once mixed requires a curing time which means silicone is viscous during the printing process which can result in deformation of the structure at best and complete structural failure at worst.

1.2 Importance of the Study

As a material 3D-printed silicones have a lot of potential due to its desirable properties compared to conventional materials such as plastics and metals for household products. Aside from this, as a material it is more in line with modern living standards as it can be used to create products with ergonomic designs, it is sustainable, and the usage of 3D-printing makes it highly customizable. However, silicone is underutilized in household applications, this is mainly due to the lack of research and innovations into the potential of silicone outside of basic applications such as handles, containers and seals. Using 3D printing, new innovations and designs can easily be studied by universities and private research companies.

1.3 Problem Statement

Despite the growing interest in 3D-printed silicones within the scientific community for biomedical and industrial sectors, there is still a lack of research and development into household applications. The lack of research can be attributed to the focus on biomedical and industrial sectors as 3D-printed silicones have great value in robotics and medical applications. Aside from this, there is also a growing demand from consumers for modern products that are also eco-friendly which can be accomplished by through the combination of silicones and 3D printing. Other materials such as plastics and metals have limitations that have to be constantly worked around such as poor recyclability for plastics and limited flexibility, and heavy mass for metals. Due to these gaps, the potential and benefits of combining silicone's material advantage and additive manufacturing remain untapped. There is an opportunity to address the research gaps on innovation in daily-use household products.

1.4 Aim and Objectives

The aim of this study is to evaluate the potential suitability of the 3D-printed silicones as a cushioning material in sofa cushions and understand how different infill patterns and designs influence the mechanical properties of 3D-printed silicone samples. The objectives of this study are listed below:

1) To compare the mechanical properties of 3D-printed silicones to conventional household cushion materials.
2) To design and fabricate prototype samples of 3D-printed silicones with different infill patterns and designs.
3) To evaluate the effect of different infill patterns and designs on the material usage and mechanical properties (stress-strain relationship and Young's Modulus) of 3D-printed silicone cushions.

1.5 Scope and Limitation of the Study

As there are many variables that can be studied when it comes to 3D-printed silicones, this study is limited to one type of silicone to ensure the focus of the study is on the printing patterns and infill design. This will ensure that the results and manipulated variables are constrained to the printing parameters rather than material variation.

Aside from this, the duration of the study is limited to at most 6 months of study to test the durability and longevity of the prototype. The total length of the study across 3 semesters only lasts one year which prevents long-term durability testing on the prototypes. The ability to study the long-term effects of the environment and constant usage on the product is crucial as it would provide beneficial data to better understand the viability of the prototype as a replacement for currently used materials in sofa cushions.

This study is also constrained to using Direct Ink Write method of 3D-printing due to the availability of 3D printer within the university.DIW is a simple and straightforward 3D-printing technique that will allow to the 3D-printing of silicone elastomers that can maintain its elastic properties. Other methods such as vat polymerization and embedded 3D-printing require specialized equipment, more advanced knowledge, and specific materials to maintain elastic properties.

The available 3D-printer is unable to produce full scale prototypes which simplifies the testing process and apparatuses. This allows for simpler to conduct testing methods which reduces the amount of time and effort needed to plan and build the necessary apparatuses. Unfortunately, the downside of small-scale prototypes is that potential differences or challenges that may occur when scaled to full sized prototypes will not be included in this study. Due to scale law, these potential differences may cause major deviations in data and results as certain parameters may increase or decrease exponentially.

Lastly there is a lack of specialized equipment to conduct long-term durability testing such as repeated stretch and compression tests. The specialized equipment would require a longer study period and full-scale prototypes to properly conduct repeated stretch, and compression tests to obtain relevant and accurate data.

There is a lot of potential for future work to build upon the data from this study such as long-term durability testing, full-scale prototypes, diverse silicone formulations, and alternative 3D-printing methods.

1.6 Contribution of the Study

This study shows the potential of 3D-printed silicones to replace conventional cushioning materials. It shows the importance of further research and development into the usage of 3D-printed silicones for household usage. The development of 3D-printed silicones into cushioning material can greatly increase the longevity of the products and it can be customised to better fit the ergonomics of individual consumers. By testing the physical and mechanical properties of 3D-printed silicones, it shows the potential for further research into this field and optimisation through different 3D-printing technologies, silicone formulations, and printing parameters.

1.7 Outline of the Report

This report is separated into 5 Chapters as shown below:

Chapter 1 – Introduction

Introduces the background of the study, problem statement, objectives, aim, scope, limitations, and the significance of the project.

Chapter 2 – Literature Review

Presents the literature review regarding the 3D printing methods for silicone, infill patterns and designs, and sustainability of silicones.

Chapter 3 – Methodology

Describes the methodology used in this study, including silicone formulation, printing parameters, compression testing methods, and data analysis methods.

Chapter 4 – Results and Discussion

Discusses the results obtained and provides analysis and interpretation of the findings.

Chapter 5 – Conclusion

Concludes the results of the study and provides recommendations for future work in this field.

CHAPTER 2

LITERATURE REVIEW

2.1 3D-Printing Methods for Silicones

Additive manufacturing or more commonly known as 3D-printing is a general term to refer to manufacturing techniques that involve addition of material compared to traditional manufacturing techniques which involve the removal of material to form the desired object or shape. This more modern process allows for intricate and specially designed internal structures to be easily manufactured even in small objects which would have been very hard or near impossible using traditional subtractive methods.

According to Al'aref et al., (2018) one of the first published research papers on additive manufacturing was conducted in the 1960s at Battelle Memorial Institute in Ohio which was on using two laser beams with different wavelengths to polymerize resin at the intersection of the beams. Following this, in 1980, Hideo Kodama developed one of the first rapid prototyping techniques only using a single laser beam that would eventually be fully developed and patented by Charles Hull with the invention of stereolitography in 1984 (Al'aref et al., 2018).

Nowadays the general understanding of 3D-printing refers to fused deposit modelling (FDM) which involves extrusion material in the form of a polymer filament through a heated nozzle which heats and melts the filament and deposits it layer by layer to create the 3D object (Sharma, Dhanopia and Joshi, 2020). This is due to the influx of commercial desktop 3D printers by companies such as Bambu Lab, Creality and Ultimaker which spawned a large community across the world who share designs and tips on social media.

Despite the simplicity and availability of 3D-printer that use FDM there are other methods that are frequently used in industrial and research applications according to Al'aref et al., (2018) which include Selective Laser Sintering (SLS), Direct Write (DW), Stereolithography, and Material Jetting (MJ). However, due to silicone's thermoset properties and being initially being a liquid before curing, the options available for 3D-printing silicones are more limited compared to other materials like plastics.

The simplest method is similar to FDM as it is also an extrusion based printing method which is referred to as Direct Ink Writing (DIW). The difference between them is that in DIW the material used is a viscoelastic material which has either an elastic(solid-like) or viscous(liquid-like) property as this will allow the material to flow when experiencing shear forces (Al'aref et al., 2018). This property negates the necessity for a thermally induced phase change which is used in FDM when the material is heated to allow it to flow out of the nozzle. For silicones specifically, usually a syringe with the mixed uncured silicone will act as the nozzle and the feed rate of the print is controlled by the force applied on the plunger.

Despite its simplicity, the DIW method does come with technical difficulties which according to Zhou et al. (2019) are: (1) Limited material choice as silicones that have low viscosity and slow cure time are unsuitable for DIW despite any other beneficial properties. (2) Short printing time as fast curing silicones have a short amount of time where the mixed silicone is still viscous enough to be printed with before solidifying. (3) Fixed printed fiber resolution as they are typically fixed due to the size of the nozzle and are not usually changed once the printing process has started. This prevents the usage of dynamic printing parameters when it is beneficial.

Next method is referred to as vat polymerisation printing (VPP) where light is used to cure a layer of liquid polymer resin then the print bed is moved up or down for the next layer to be cured, thus creating the 3D structure (Hurlbutt, 2024). Vat polymerisation printing is a broad term to refer to additive manufacturing techniques that involve the curing of a layer of resin in a vat of liquid resin. Due to this both stereolitography and Digital Light Processing (DLP) are considered vat polymerisation methods (Hurlbutt, 2024). According toWong, Ganguly and Tang (2024) VPP has very high resolution and printing accuracy alongside good surface quality as the printing parameters are not fixed from the start of the printing process and can dynamically adjust to suit specific scenarios when certain characteristics are more desirable.

DLP differs from stereolitography as in DLP, UV light is shined on the vat of resin to cure an entire layer at once whereas stereolitography uses a focused beam of UV light instead. This characteristic of DLP enables a very fast printing time compared to stereolitography (Zhao et al., 2019) which is highly desirable in industrial applications to enable mass production of products.

Inkjet 3D printing is a relatively new technique when it comes to 3D-printing silicone as the oldest research paper found regarding this technique is from McCoul et al. (2017). It mirrors the technology currently used in normal printers by directing droplets of fluid(ink) onto a substrate to form patterns (Farid Bensebaa, 2013). Śliwiak et al. (2021) developed a print head that uses inkjet technology to 3D print a type of reactive silicone that has a wide variety of applications. By ejecting two droplets of ink that will mix in free space and undergo rapid polymerisation, high speed and high resolution 3D-printing using inkjet technique can be achieved (Śliwiak et al., 2021).

So far the 3D-printing methods are either applying material onto a substrate with inkjet and DIW or selectively curing shapes from a liquid vat with vat polymerisation. Embedded 3D-printing is a combination of both methods where the nozzle is embedded in a support matrix or bath in which it will print continous filaments within the support matrix which allows for printing using ink that are not printable using extrusion based techniques as stated by Friedrich and Woodcock (2025). Embedded 3D-printing is also able to print structures that require support without adding the supports in the print itself as the support matrix allows for the printed object to be suspended within the matrix itself. This technique allows for a greater variety of shapes and complex geometries to be printed without supports.

2.2 Infills

When designing a 3D-printed part, one of the printing parameters that must be considered carefully is the infill percentage and pattern. Infill refers to the internal structure of the 3D printing part which can be designed and set to a specific percentage volume filled as one of the printing parameters. It is important to consider as it will affect the weight, amount of material usage, structural strength and printing time (Naoum and Piccoli, 2022).

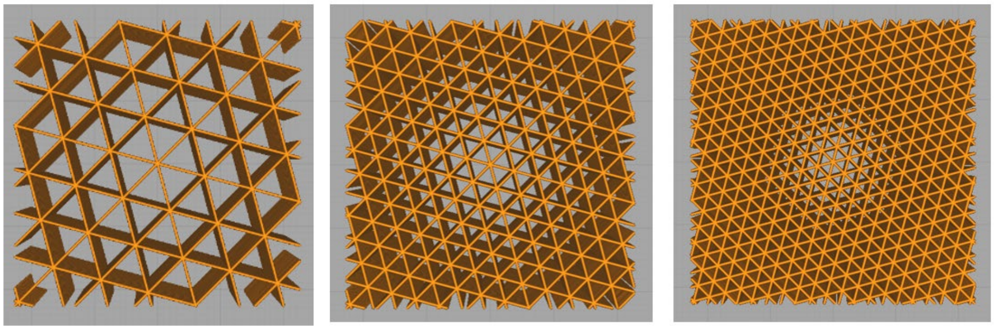

(a) (b) (c)

Figure 2.1: Triangle pattern infill with different infill percentages, showing (a) 20%, (b) 40%, (c) 60%.

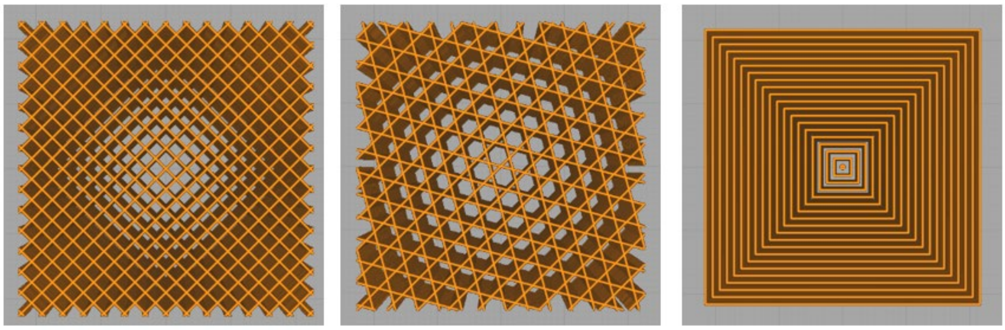

(a) (b) (c)

Figure 2.2: 40% infill of different patterns, showing (a) grid, (b) tri-hexagons, (c) concentric.

It is usually undesirable to print a design with complete infill which would mean the printed part is completely solid as the use case may not need that much structural strength. The flexibility of 3D-printing being able to design specific patterns and percentages for the infill of an object allows it to reduce in material cost while maintaining necessary structural integrity and modification of the structural characteristics. This flexibility contributes to the sustainability of 3D-printing compared to other manufacturing techniques.

In the case of elastomers like silicone, infill patterns and percentages not only determines the structural strength of the 3D-printed part but also the elasticity of it. By modifying the infill percentage and patterns, the characteristics of the silicone part can be adjusted to suit different applications and even have different areas of a single part to exhibit different material characteristics.

2.3 Sustainability of Silicones

One of the main concerns when it comes to the implementation or adoption of a new material is it's sustainability as the global focus on green technologies has grown exponentially since the Paris Agreement in 2016. As discovered by Wolf and Stammer (2024), silicone use as a material results in a reduction in greenhouse gas emissions and energy savings which are able to exceed the manufacturing impact and end-of-life disposal up to a factor of nine. This shows the potential of silicone to positively impact the environment if used to replace other materials such as plastics. Despite this there is still the issue of disposal when silicone products reach their end-of-life as silicone is not biodegradable and recycling centres for silicone products are scarce compared to recycling centres for plastic, or metals.

According to Wolf and Stammer (2024), due to the non-biodegradability of silicone, incineration has become the preferred method of disposal of waste silicone instead of disposal in landfills. However, this will still result in the loss of material silicone and the energy used to produce it. As such companies have begun to look into expanding the chemical recycling of silicone and establishing a closed loop system for silicone (Wolf and Stammer, 2024). The ability to recycle silicone is especially important eventhough it is non-toxic and considered biologically inert (Ottenbrite and Javan, 2005), because once a silicone product breaks or rendered unusable it is unable to be repaired or reformed due to the inert nature of silicone causing any attempted repairs to introduce new weak points and possibly compromise the structural integrity of the product.

The main goal when it comes to recyclying silicone through chemical means is the breaking of the siloxane (Si-O) bonds which is the main backbone of the silicone chemical structure that give it's polymer characteristic. However this is difficult to achieve as the siloxane bonds are very strong and chemically inert which can sustain heating of 200 °C up to a year and up to 450 °C for a short period of time (Buddhima Rupasinghe, 2023). Despite this difficulty there are a few methods that enable the breaking of those bonds and allow for the recycling of silicone products

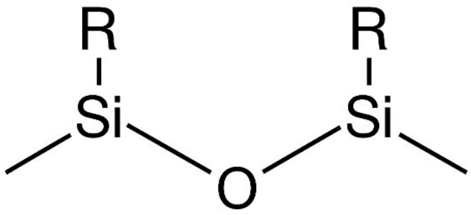

Figure 2.3: Siloxane Bonds.

Firstly through chemical methods, depolymerisation is possible through the addition of acids or bases. Buddhima Rupasinghe (2023) found that acids used include sulfuric acid, triflic acid, and hydrofluoric acid, while some other groups used strong bases such as amines, octanoate catalysts, and organotin carboxylates. Through this method, the silicone waste is depolymerised into oligomers which can then in turn be repolymerised into new products and even enables upcycling by turning the waste into new, higher value products (Wolf and Stammer, 2024). Theoretically this should enable the closed loop of new silicone products turning into waste after usage and recycled back into new silicone products. This would optimally be the best option for sustainability but there are challenges faced when processing it such as the necessity for highly efficient filters, separation of monovalent units and/or trivalent units from divalent units, separation of catalysts, and removal of gaseous impurities.

There is also mechanical recycling of silicone, where silicone waste is converted into fine particles a series of operations to breakdown the physical size of the silicone waste that involve shredding, grinding, crushing and milling (Wolf and Stammer, 2024) then mechanically incorporating the grounded silicone particles into new virgin material. Although the process requires lower energy compared to chemical recycling, Wolf and Stammer (2024) found that new silicone products manufactured this way would have worse mechanical properties compared to virgin silicone due to contaminants from the silicone waste compromising the quality. Due to these reasons, mechanical recycling is not suitable as a long-term solution to the recycling and sustainability of silicone products.

Aside from the recyclability of silicones, it can also be used in other ways to replace less sustainable and more toxic materials. Fouling refers to the growth of animals and plants on sea structures or ships which can increase the fuel consumption of ships (Fitzsimons and Parry, 2009). According to Lagerström et al. (2022), a biocide-free silicone based foul-release coating performed better than the alternative biocidal antifouling coatings. This shows the potential for silicone based products to replace currently used materials as a more sustainable alternative.

2.4 Cushion Performance

The type of material used to provide cushioning support in everyday household items such as sofas, beds, and pillows is very important to provide adequate support to hold up the weight of the user, while also being soft and feeling comfortable. To ensure that a new material is suitable to be a cushioning material, a few factors can be analysed to better understand and evaluate its performance characteristics.

Notable performance metrics include support factor (SAG), stress-strain relationship, Young's modulus, and energy absorption capabilities. Each of these factors shed light on different aspects of the mechanical properties of the cushioning material. Support factor shows comfortability, stress-strain relationship allows prediction or expectation of the materials mechanical response, Young's modulus shows how stiff the material is, and the energy absorption capabilities show how much energy the material is capable of absorbing.

3D-printed silicones has a unique capability to modify mechanical properties through both infill design and architecture, and material characteristics using different silicone formulations. Rodriguez et al. (2021) were able to develop a series of UV-curable silicone elastomers that had tunable mechanical properties which changed the . Aside from this the lattice structure was found to play a key role in controlling the mechanical behaviour such as Young's modulus, energy absorption capacity and strain recovery (Beloshenko et al., 2021). This shows the versatility of 3D-printed silicones to produce different mechanical properties depending on user needs and markets all while retaining the same production line little to no modification needed to the machinery.

The benefits of using 3D-printing for cushion material can be seen from a study done by de la Rosa et al. (2024) where 3D-printed thermoplastic polyurethane was used to produce a personalised pressure cushion for a patient by changing the lattice structure at different zones of pressure to improve support while also reducing material usage. The customisability shows the potential for specialised cushion materials and design that can better fit to the ergonomics of customers while simultaneously reducing material usage.

CHAPTER 3

METHODOLOGY AND WORK PLAN

3.1 Introduction

This study focuses on using quantitative tests to understand the viability of 3D-printed silicones as a replacement for conventional cushion materials. Throughout this study, some of the apparatuses used include universal testing machine and modified 3D-printer for silicone. The test included within this study include stress-strain test using compressive testing. Using these testing methods, an accurate understanding of the 3D-printed parts' mechanical characteristics and durability can be obtained and thus compared with conventional materials.

The 3D-printing method used will be direct ink writing due to the availability of the 3D-printer and the simplicity of operation compared to other printing methods. Each part of the process from the preparation of the silicone mixture to the analysis of data.

3.2 Silicone Preparation

The silicone formulation has a base of polydimethylsiloxane (PDMS) which is the standard form of silicone and typically used in formulations for 3D-printing purposes (Ryszczuk et al., 2026). The chemical composition of a monomer of PDMS is shown below:

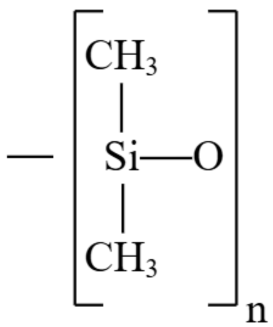

Figure 3.1: PDMS Monomer

The PDMS mixed with nanosilica crystals to improve its rheological characteristics. Without the addition of nanosilica crystals, the printed silicone mixture will continue to flow and spread out which will compromise the shape of the printed filament. The addition of nanosilica as described by Truby et al. (2018) was found to modify the rheological characteristics by causing the non-Newtonian fluid to exhibit shear-thinning behaviour. This means that the viscosity of the fluid decreases as stress applied to them increases which ensures the shape of the printed filament to remain.

By adding nanosilica crystals the shape and quality of the printed silicone part can be maintained during the curing process. The silicone formulation will not change throughout the study to ensure the focus is on understanding the effects of the design of the infills, infill percentage, and printing parameters on the physical and mechanical properties. The silicone formulation for a single batch is as shown below:

Table 3.1: Silicone mixture components and amount.

Component	Amount
PDMS	30 g
Silicone oil	4.87 g
Slow crosslinker	3.24 g
Fast crosslinker	0.36 g
Nanosilica	2.5 g
Catalyst	1 drop

To prepare the silicone mixture disposable equipment is used due to the cured silicone being very hard to clean out so it is preferable to dispose of the mixing container. The equipment used includes a disposable plastic cup, single-use chopsticks, a plastic scraper, a 20 ml luer lock syringe, overhead stirrer, and a weighing balance.

The disposable plastic cup was placed on the weight balance and the components are added in the order shown in Table 3.1 from top to bottom into the disposable plastic cup and is mixed using the chopsticks after every component was added. Since the slow crosslinker, fast crosslinker and catalyst are in liquid form and kept in a syringes, is is important to push some material out onto tissue paper as it may harden at the head of the syringe causing lack of control when dispensing the material as the amount needed is very small

Once all the components are added together, the mixture is stirred using the overhead stirrer at 300 RPM to ensure a homogeneous mixture. It is very important to ensure that the mixture is homogeneous, as the rheology of the mixture needs to be consistent to hold up to shape during printing, and the crosslinkers need to be thoroughly mixed to ensure the final part cures properly and completely.

Once the silicone mixture is completed, it is transferred into a syringe by removing the plunger and using the plastic scraper to push the silicone into the syringe. The syringe acts as a repository for the silicone material during the printing process. Each batch can be used to fill a whole syringe which will be around 20 ml but due to the viscosity of silicone, there will be some air bubbles within the syringe. These air bubbles will not be an issue as when the plunger is pushed, the air bubbles will escape out of the syringe first before the silicone flows out of the nozzle.

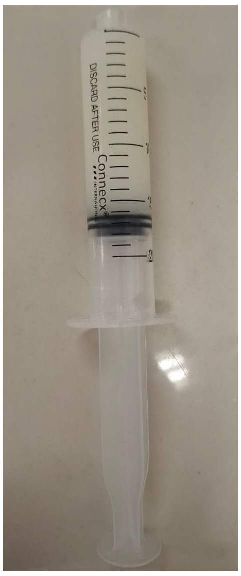

Figure 3.2: Silicone Mixture in the Syringe

After the syringes are filled, if they are not used in the same day to print out any samples, they will be kept in a freezer to ensure the silicone does not cure within the syringe. The same will be done if there is any leftover silicone after printing. When kept in the freezer, the silicone mixture can be kept for 3 – 4 days without any issue. Longer than that, partial curing of the silicone mixture can occur which will make the batch unusable.

3.3 Printer Setup

The printer used is a modified Enders 3 printer where the printing head was removed and replaced with a motor with a worm gear is attached to the frame to push the syringe in a controlled manner for precise deposition of silicone and a holder for the nozzle. The first step to setting the printer up for use is the syringe filled with the silicone mixture will be attached to tubing and an 18G nozzle which acts as the printing head using metal fittings. The tubing is around 40 cm long to ensure it has enough slack as the printing head moves.

The syringe is placed in the receptacle then the tubing is curved and nozzle is placed into the holder. Due to the size of the nozzle holder and the fitting size being slightly different, the fitting may not be able to fit into the nozzle holder. To address this issue, a piece of paper is folded multiple times or masking tape can be wrapped around the metal fittings to increase the thickness. This simple fix allows for the fitting to be secured properly in the holder. As can be seen below it is important that the tubing is curved from the left to the right to ensure the tubing can move with the nozzle and not interfere with the syringe during printing.

Figure 3.3: Syringe Setup for the Printer

The next step is to ensure the bed is level and the distance between the nozzle and the bed is correct. A plastic film is placed on bed and secured with a binder clip so the silicone samples can be moved to a different location for curing. A piece of paper is placed on top of the plastic film and the nozzle is adjusted close to the bed, and the printer head is moved to the closest corner of the bed. The bed height is adjusted using the gears at the corner of the bed until the tip of the nozzle catches the sheet paper. This is repeated at each corner of the bed to ensure uniformed level across the whole bed.

Once the levelling is complete, the auto home function is used and the height of the bed and the nozzle are not adjusted any further for the rest of the printing process. The extruder is activated and used to slowly compress the plunger of the syringe to push the silicone all through the tubing and nozzle. It is important to do this slowly because the internal pressure will build up if done too fast. This build up in pressure can cause the plunger to deform and the motor to not spin properly which can cause damage to the equipment used. Once the silicone begins to flow out of the nozzle, the printing of the samples can be proceeded with.

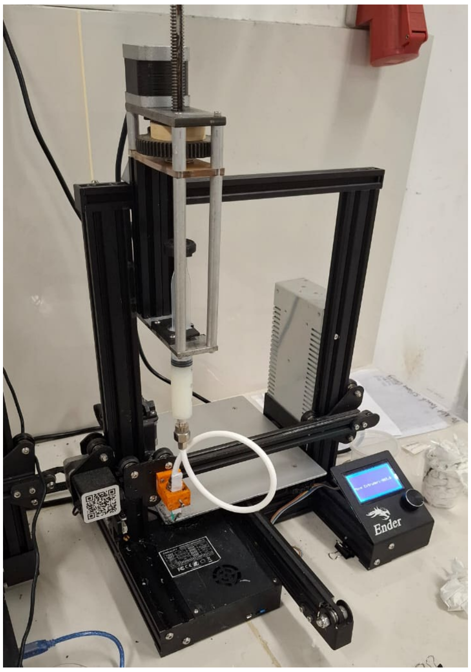

Figure 3.4: Full Printer Setup

3.4 Printing of the Samples

Before the samples can be printed, the 3D models and gcode for each sample needs to be prepared. The samples follow ASTM D575 standard, with the testing samples of cylindrical disk shape with dimensions of 28.5 mm in diameter and 12 mm height. For complex shapes and designs, usually the model is prepared in a 3D modelling software such as SolidWorks before being imported into a slicer software to prepare the gcode for the 3D printer and adjust printing parameters. However, due to the simplicity of the samples' shapes, it was directly modelled in the slicer software before slicing.

The slicer software used is Prusa Slicer as this was the slicer software used by the postgraduate student handling 3D-printed silicones, has an easy to use user interface (UI) and features that are desirable. It can be used to quickly check the material usage, cut through the layers, and make it easy to visualise the different parts of the printed part directly in the software. The slicer settings and preview of Prusa Slicer are as shown below:

Table 3.2: Slicer Settings.

Layer Height	0.4 mm
First Layer Height	0.4 mm
Skirt Loops	5
Distance from Brim	2 mm
Skirt Height	1 layer
Speed	10mm/s
Vertical Shells	1
Horizontal Shells	0

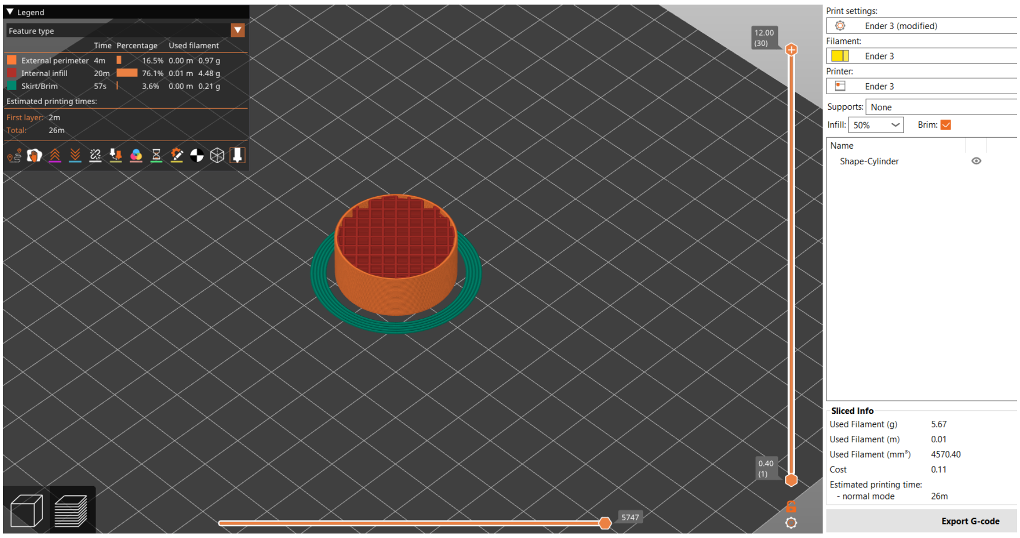

Figure 3.5: Prusa Slicer UI.

No horizontal shells were used, as they could alter the stress-strain relationship and affect the final experimental results. The number of vertical shells were set to one to ensure the minimum effect on the stress-strain relationship of the sample. The vertical shell is important to maintain the shape of the print as without it, the samples will collapse onto itself and the silicone will not deposit properly throughout the printing process. 5 skirt loops are added to ensure the flow of the silicone reaches steady state before printing the part itself. The speed was set to 10mm/s as it was found to be the best standard speed by the postgraduate student, but it can still be increased or decreased during the printing process if needed.

The 4 infill patterns used were Grid, Gyroid, Stars, and Triangle with infill percentage of 40% to 70% in intervals of 10%. These infill percentages were chosen as there is a practical limit to the minimum allowable infill percentage that can be printed using silicone before the printed part will fall apart due to its own weight and lack of support. Lower infill percenatages were also found to have higher rate of defect during printing as small print head movement errors are exacerbated when the infill percentage is lower. During preliminary testing, this limit is found to be around 30% – 40% depending on the infill pattern. Aside from this, 80% - 100% were also not used as the printed part will be very stiff, and would have properties more similar to a full silicone part which defeats the purpose of studing the 3D-printed characteristics. A total of 16 samples were printed as 4 infill patterns having each 4 different infill percentages. The infill patterns are shown below:

Table 3.3: Top Down View of Infill Patterns.

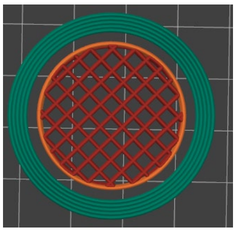	Grid	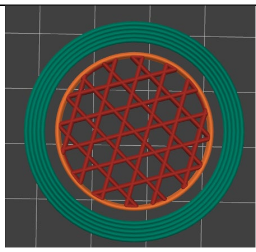	Stars
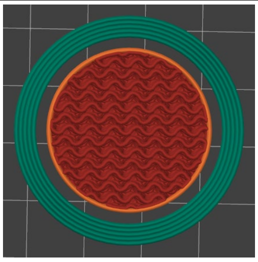	Gyroid	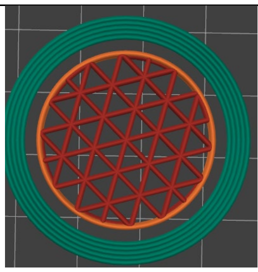	Triangle

Once the dimensions, infill patterns, and percentages are set, the gcode is exported and transferred to an SD card that can be directly read by the 3D-printer and the printing of the samples can begin. Throughout the printing process it is important to continuously watch the sample be printed to look out for any defects or issues with the gcode. By watching the print, it can be stopped early and adjusted to prevent wastage of material since it takes around an hour to mix a batch of silicone and put into the syringe. Understanding how defects occur is also very important so the parameters or movement of the print head can be adjusted to reduce the defects that can occur. Following these steps, all the samples were printed out and can be seen below:

Figure 3.6: Printed Silicone Samples.

3.5 Compression Test

The testing methodology is based on ASTM D575 (Standard Test Methods for Rubber Properties in Compression) Test Method A (Compression Test of Specified Deflection) as there is no specific standard for testing 3D-printed silicone products. The compression test was carried out using a Shimadzu Autograph AGS-X universal testing machine rated for 100kN max load. The samples were subjected to compression at a rate of 4mm/min to a maximum displacement of -8mm which is around 67% strain. The force, displacement, stress and strain were recorded. The universal testing machine has the proprietary Trapezium X software which can adjust the testing parameters, and record various sets of data for analysis later on.

This software produces a report for the stress-strain graph, maximum stress, and maximum force which is used for comparison with reference data. The machine records data every 0.01 seconds to provide accurate data throughout the compression test. The data obtained was also exported out in CSV files for further analysis and comparison using Microsoft Excel. The universal testing machine used can be seen below:

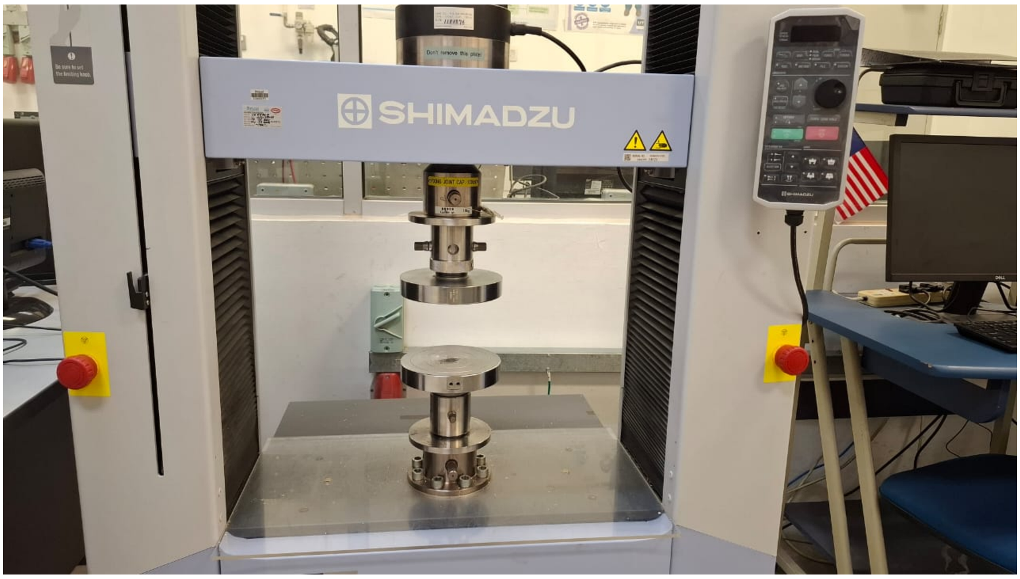

Figure 3.7: Shimadzu AGS-X Universal Testing Machine

Each sample is placed into the holder and it is lowered until a force detected by the machine, then the stroke and force are set to zero and the test is started. This is repeated on each sample to obtain results.

3.6 Analysis of Data

Using the data obtained from the compression tests, the stress-strain relationships of the samples of different infill patterns and percentages will be compared with conventional cushion materials with a focus on rubber latex foam. Microsoft Excel will be used to analyse the data to obtain elastic modulus and compile graphs for easy visualisation. The analysis of data include SAG factor, elastic modulus, and comparing material use of different patterns and percentages

CHAPTER 4

RESULTS AND DISCUSSION

4.1 Stress-Strain Relationship

The first step to understanding a material's physical and mechanical properties is to analyse the stress-strain relationship of the material. From this we can identify the different properties such as modulus of elasticity (Young's Modulus), elastic and plastic regions, and toughness of the material. The stress-strain characteristics for the different infill patterns and percentages are shown below:

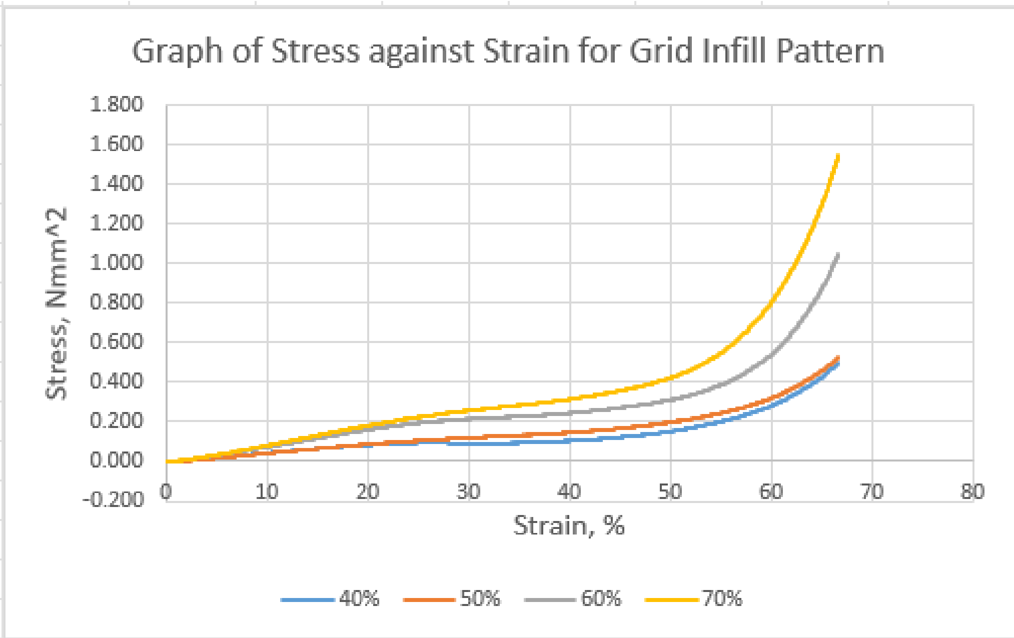

Figure 4.1: Stress-Strain Graph of Different Infill Percentages for Grid Infill Pattern

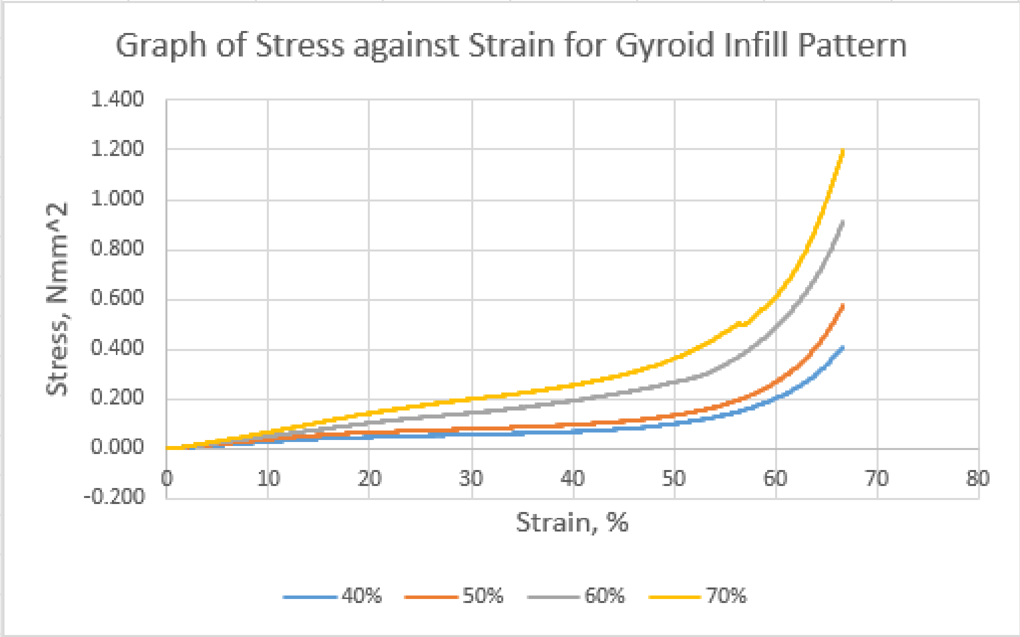

Figure 4.2: Stress-Strain Graph of Different Infill Percentages for Gyroid Infill Pattern

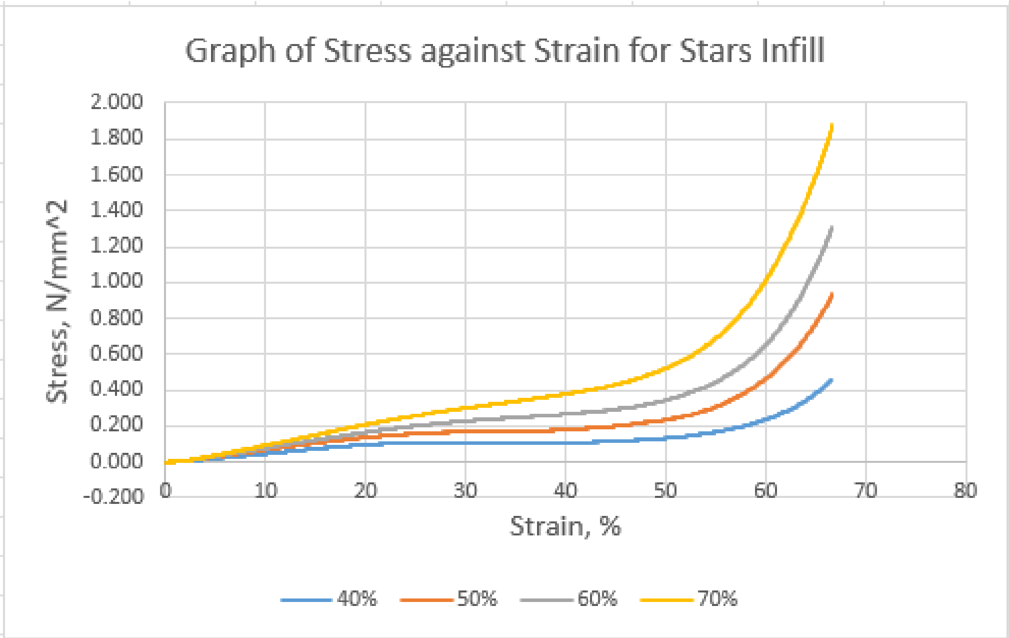

Figure 4.3: Stress-Strain Graph of Different Infill Percentages for Stars Infill Pattern

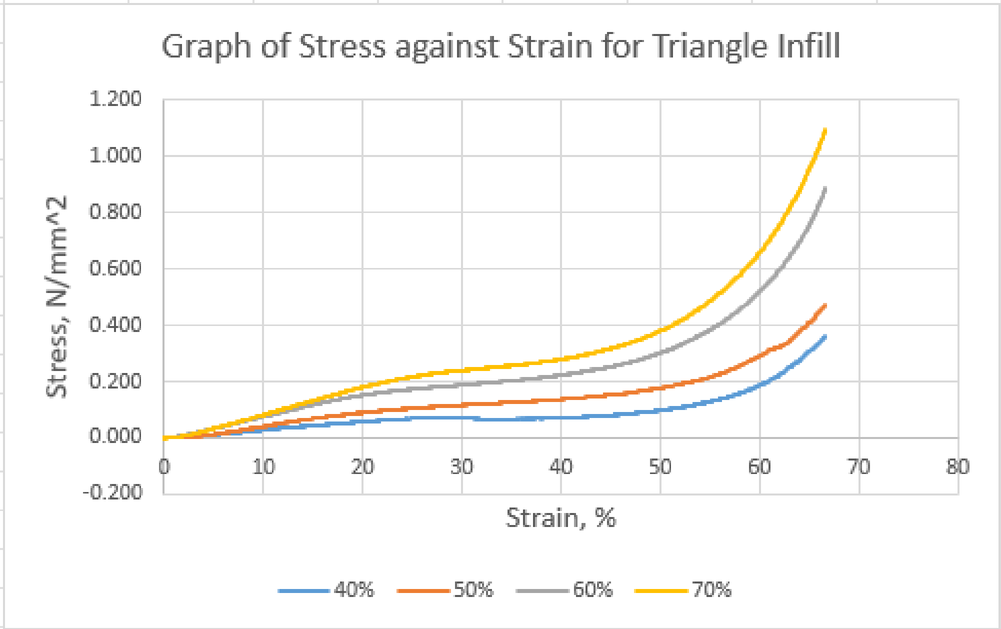

Figure 4.4: Stress-Strain Graph of Different Infill Percentages for Triangle Infill Pattern

For the stress-strain relationship for grid infill, it can be seen in Figure 4.1 that the relationship for 40% and 50% are quite similar to each other with 50% having a only slightly higher stress response. There is a notable increase in stress response from 50% infill to 60% infill compared to the rest of the graph. This implies that there is a much larger change between 50% and 60% compared to the rest of the different infill percentages. The graph can be divided into 3 different areas: first area between 0% to 20% strain, second at 20% to 50% strain, and finally 50% to 70% strain. The first region has a linear stress response, then it plateaus in the second region, finally transitioning into a much steeper response in the third region. These 3 regions show the tactile feedback that will be experienced by a user it is compressed.

These 3 regions can be explained as the direction of force is the same as the direction of printing which means the force is transferred directly into the vertically printed internal structure. The grid pattern, as can be seen from Table 3.3 the pattern in the y-direction is composed of straight walls. When a long and slender component experiences a compressive vertical force, buckling can occur whereby the component suddenly deforms in the axis perpendicular to the force. Buckling occurs as no component can be perfectly straight and loading on the component will never be perfectly in a single axis, thus leading to the component suddenly deflecting (Donnelly, 2020).

According to Boresi & Schmidt (2003) sudden lateral deflection will occur when the compressive load reaches the critical buckling load which can be seen below:

$$P = \frac{EI\pi^2}{L^2}$$

where:

P = Critical Buckling Load

E = Young's Modulus

I = Moment of Inertia

L = Length of Component

Once buckling occurs, the stress response of the component may change which accounts for the change from the first area to the second area as seen in Figure 4.1. The third area occurs when most of the silicone material has been compressed, most of the air in the internal structure has been pushed out, and the internal structure's stress response is not due to buckling but rather the surface area of the internal structure that experiences the loading. At this point the stress response increases rapidly and most of the support from the material will occur at this region and it is referred to as densification.

These 3 region response also occurs for the triangle and stars infill pattern as all 3 of these infill patterns have a design where by the internal structure is composed of vertical walls in the same direction as the applied load. This implies that to obtain different stress-strain relationships, the infill pattern cannot be solely composed of vertical walls in the direction of the applied load. As can be seen in Figure 4.2, the gyroid infill pattern has the smoothest relationship from 0% to 50% without much visible change in the graph to separate into 2 different regions. Gyroid has the most unique design as it is a triply periodic structure which are mathematical structures that exhibit three-dimensional periodicity (Zhang et al., 2018). Three-dimensional periodicity means the structure can be repeated in any direction until infinity and thus has the same structural properties in all directions. Due to this characteristic the internal structure avoids the sudden change in stress response due to buckling.

Both gyroid and triangle share a similar characteristic to the grid pattern where the 50% and 60% infill percentage have a large change in stress response compared to 60% to 70% and the 40% to 50% infill percentage. The stars infill pattern is different as the 50% and 60% infill percentage have a change in stress response whereas the 40% to 50% and the 60% to 70% have a much higher change in stress response.

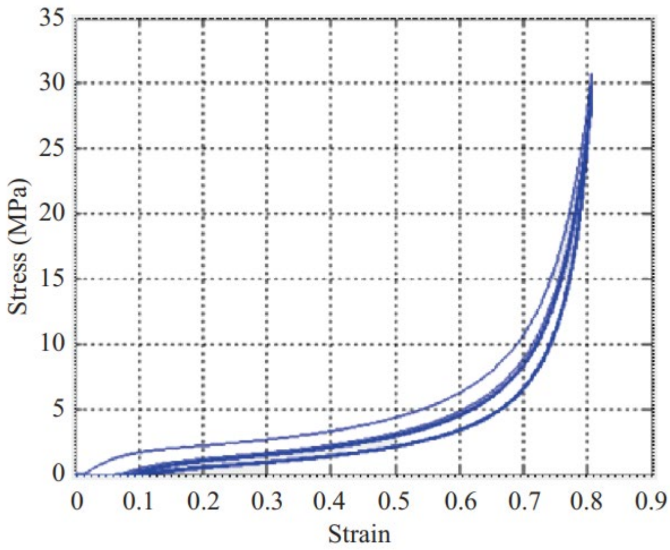

Figure 4.5: Stress Strain Curve of EVA Foam. (Liu et al., 2016) Reprinted with Permission from Copyright 2016 Oxford University Press

As seen in Figure 4.5, the stress-strain relationship of the 3D-printed silicone samples are similar to that of EVA foam. The gyroid pattern appears to have the most desirable stress-strain response as cushioning materials should not have a smooth and consistent tactile response to it compared to the others which have multiple changes in the stress-strain relationship.

4.2 Young's Modulus

The Young's modulus also known as elastic modulus is the stiffness of a material or its resistance to elastic deformation. It can be obtained from the stress-strain graphs as stress is proportional to strain through the formula shown below (Boresi & Schmidt, 2003):

$$\sigma = E\varepsilon$$

The Young's modulus for each of the samples were obtained from the results obtained from the the testing done through the universal testing machine as can be seen below:

Table 4.1: Young's Modulus of Silicone Samples of Different Infill Patterns and Percentages.

Infill Pattern / Infill Percentage	Young’s Modulus, N/mm^2			
	Grid	Gyroid	Triangle	Stars
40%	4.13380	4.54049	3.37993	5.10654
50%	4.64031	6.55535	3.75863	9.75389
60%	10.3032	9.85195	8.08449	14.3892
70%	13.8536	14.1801	8.38469	19.8566

When comparing the different infill patterns for an infill percentage of 40%, the highest Young’s modulus is from the stars infill pattern with 5.10654 N/mm^2 which would mean it is the stiffest of all the patterns. The lowest if from the triangle infill pattern with a value of 3.37993 N/mm^2 which means it is the least stiff of all 4 patterns tested. Gyroid and grid are moderately stiff with a value of 4.54049 N/mm^2 and 4.1338 N/mm^2 respectively and have very similar values.

At 50% infill, the highest remains as stars infill pattern with a value of 9.75389 N/mm^2 which is approximately an increase of 4.65 N/mm^2 compared to 40%. The lowest is also still triangle at 3.75863 N/mm^2 which is a very small increase of only around 0.68 N/mm^2. Gyroid has an increase of around 2 N/mm^2 to 6.55535 N/mm^2, while grid also had a very small increase of less than 1 N/mm^2 to 4.6301 N/mm^2.

For 60% infill, the highest Young’s modulus is the same with stars pattern with a value of 14.3892 N/mm^2. The lowest also stays the same with triangle pattern at 8.08449 N/mm^2. Gyroid and grid, are still in the middle with Young’s modulus values of 9.85195 N/mm^2 and 10.3032 N/mm^2. At this infill percentage, the Young’s modulus values increases substantially across all the infill patterns. The gyroid pattern also goes from second highest value to the third highest value due to grid pattern having a very high increase of around 5.7 N/mm^2. The average increase across the different patterns is around 4 N/mm^2.

Finally, for 70% the overall relationship remains the same, stars is the highest with 19.8566 N/mm^2. Triangle pattern has the lowest of 8.38469 N/mm^2, which is a very low increase of only 0.3 N/mm^2. Gyroid returns to be the second highest with a value of 14.1801 N/mm^2 and grid has a value of 13.8536 N/mm^2.

From Table 4.1 it can be seen that 60% infill has the highest increase from each interval of 10%. Triangle pattern for 40% and 50%, and 60% and 70% are very similar with differences of less than 0.5 N/mm^2. Grid also has a significant increase from 50% to 60% while the difference between 40% and 50%, and 60% and 70% are much smaller.

Direct comparison of Young's modulus for cushioning materials is impossible as there can be many different types of materials that are used and even the same company would use different materials to manufacture different types of product for different uses. However, cushioning materials will have a low Young's modulus According to Gent & Thomas (1959) the Young's Modulus of rubber latex foam is 2.54873N/mm^2. As seen from Table 4.1, the Young's modulus of all the infill patterns and percentages are low. All the samples have a low Young's modulus especially for 50% infill. Gyroid pattern looks to be attractive due to its moderate and consistent increase in Young's modulus across the different infill percentages as this would make it much easier to control the stiffness of the material when designing products.

4.3 SAG Factor

Aside from just the Young's modulus, there is another quantifiable factor that is used to better understand seating comfort which is referred to as the support factor (SAG factor). According to Silva et al. (2024) the SAG factor is a dimensionless value that is defined as the ratio of compressive load at 65% strain to the compressive load at 25% strain as can be seen below:

$$SAG = \frac{F_{65\%}}{F_{25\%}}$$

It was found by Ebe & Griffin (2001) that a higher SAG factor correlates with better comfort. To better understand what SAG factor means to a user, Moon et al. (2020) states that a high SAG factor denotes a high resistance to bottoming out. If a cushion material bottoms out, a user will not feel support from the cushion but rather the support structure that the cushioning material is placed on. Bottoming out is extremely undesirable when selecting or designing a cushioning material as it would be inefficient at cushioning and supporting body weight.

Table 4.2: SAG Factor of Samples with Different Infill Patterns and Percentages

Infill Pattern / Infill Percentage	SAG Factor			
	Grid	Gyroid	Triangle	Stars
40%	4.4	6.4	4.4	3.6
50%	4.3	6.3	3.9	4.9
60%	4.5	6.0	4.4	5.4
70%	5.8	5.8	4.4	6.2
Average	4.75	6.125	4.275	5.025

The SAG factor for grid across the 4 infill patterns of 40%, 50%, 60%, and 70% were 4.4, 4.3, 4.5, and 5.8, respectively. On average the SAG factor for grid infill is 4.75. The SAG factor for grid infill is almost the same until 70% infill where it increases by 1.3 compared to 60% infill. Gyroid pattern has the highest SAG factor with an average of 6.125 and is quite consistent. The SAG factors for each infill percentage are as follows; 40% is 6.4, 50% is 6.3, 60% is 6.0, and 70% is 5.8

The triangle infill pattern has the lowest SAG factor with an average of 4.275 and is the most consistent throughout the different infill percentages as the SAG factor for 40%, 60%, and 70% are the same at 4.4 with only 50% was 3.9. The stars infill pattern undergoes the most change as it increases between every interval. It starts with 40% at 3.6, then 50% at 4.9, 60% at 5.4, and finally 70% with 6.2 and has an average SAG factor of 5.025.

According to Ree & Kim (2026), polyurethane foam that contained cellulose fillers had an SAG of 2.5 to 3. An SAG of more than 2.8 is recommended to avoid the issue of bottoming out discussed earlier (Silva et al., 2024). As seen from Table 4.2 the SAG factor for all the tested infill patterns and percentages are higher than the recommended 2.8 which means that all the samples achieve a suitable comfort level according to the SAG factor. Gyroid has the highest SAG factor across the board and compared to the other 3 patterns tested, thus is the most desirable. However as discussed in 4.1 Stress-Strain Relationship, SAG factor is not the only factor that will contribute to a comfortable seating experience.

4.4 Material Usage

It can be easily understood that a higher amount of material used will result in a stiffer product with a higher stress response to strain. It is seen in Figures 4.1, 4.2, 4.3, and 4.4 that as the infill percentages increase, the stress response also increases irregardless of infill patterns. Material usage is also a very important aspect that manufacturers need to consider especially regarding mass manufacturing of products as material usage is directly related to to the cost and weight of the products. The infill percentages tested increase at a steady rate of 10% but the stress response seem to have major changes from 50% to 60%. By analysing the amount of material use of different infill patterns, it can shed light and provide possible explanations on the large variations that were seen in Figures 4.1, 4.2, 4.3, and 4.4 between the changes in infill percentages.

Table 4.3: Amount of Silicone used for Different Infill Pattern and Percentages.

Infill Pattern / Infill Percentage	Amount of Silicone used (mm^3)			
	Grid	Gyroid	Triangle	Stars
40%	3905.09	3733.90	3993.81	3814.54
50%	4570.40	4414.95	4247.19	4397.14
60%	5314.02	5095.31	5371.71	5092.81
70%	5929.66	5677.13	5856.27	5841.85
Average	4929.793	4730.323	4867.245	4786.585

For the grid infill pattern, the highest increase in material usage is from 50% to 60% with an increase of 743.63 mm^3 which is much more compared to the increase from 40% to 50% and 60% to 70% which average to an increase of around 640 mm^3. When comparing this material use with Figure 4.1, it implies that the much larger change in stress response can be attributed to the much larger change in material use.

For gyroid infill pattern the increase in material usage from 40% to 50% and 50% to 60% is around 680 mm^3 while the increase from 60% to 70% is only 581.82 mm^3. Unfortunately, when comparing these material usage with Figure 4.2, the material usage cannot be used to explain the much higher stress response from 50% to 60%.

The material usage for triangle infill pattern has a set of varied changes between the 4 infill percentages tested. The smallest increase was 253.38 mm^3 which was from 40% to 50%. The largest increase was from 50% to 60% which was 1124.52 mm^3 and the moderate increase was from 60% to 70% with a value of 484.56 mm^3. The very large increase of 1124.52 mm^3 from 50% to 60% can explain the large change in stress response found in Figure 4.4 while the changes from 40% to 50% and 60% to 70% are lesser.

Lastly the stars infill pattern's largest increase was from 60% to 70% which is 749.04 mm^3 while the moderate increase was from 50% to 60% which was 695.67mm^3. The smallest increase was from 40% to 50% with a value of 582.6mm^3. Similar to the gyroid pattern, the material usage does not directly correlate with the stress response found in Figure 4.3, which implies that there is another reasoning for the smaller stress response change from 50% to 60% compared to 40% to 50% and 60% to 70%.

Initially, it does not seem to make sense that the changes in material usage for the varies so much for different infill percentages despite the percentage change being linear 10% between each sample. However, due to the fixed size of the printing nozzle, and the requirement of maintaining the infill pattern despite edges of the sample may not be suitable for the pattern. For example a square cross section would fit a grid pattern very well as the outer edges can match the edge of the periodic pattern, however it would not match as well for a pattern such as stars due to the sharper angles found within the stars pattern. Thus the geometric design and nozzle cause the material usage to not necessarily increase linearly with the change in infill percentage.

As seen in Table 4.3, the pattern with the lowest average material use is gyroid with 4730.32 mm^3 and the highest material usage is from the grid pattern with an average value of 4929.79 mm^3. Triangle and stars have moderate amount of average material use with 4867.25 mm^3 and 4786.59 mm^3 respectively. From these average material usage values, it can be seen that gyroid is the most desirable as it has the lowest material use which means less material cost and lower weight.

CHAPTER 5

CONCLUSION AND RECOMMENDATIONS

5.1 Conclusion

From the research conducted, the objectives of the study were achieved successfully through design, fabrication, and testing The 3D-printed silicone samples have similar characteristics such as high SAG factor, low Young's modulus, and desirable stress-strain relationship. Based on the comparisons between the different infill patterns, the gyroid pattern has the most desirable characteristics with the highest SAG factor, moderate Young's modulus, smoothest stress-strain relationship, and also has the lowest volume of material usage.

There is no optimal infill density as the exact stress-strain response depends on the type of product intended to be produced. the results show that changing the infill percentage allows manufacturers or designers to modify the stress-strain relationship and Young's modulus by adjusting the infill percentage to fit the desired characteristics.

With further optimisation into mass production of 3D-printing silicones, there potential for replacing conventional cushioning materials with this modern that can be used to improve the quality of life for daily use.

5.2 Recommendations for Future Work

The research conducted in this study is merely the first step to optimizing both 3D-printed silicones and replacing conventional cushioning materials as this study shows the potential and proof of concept. However better optimisation in 3D-printing process and further research into design templates and optimal parameters are necessary before 3D-printed silicones can be commercialised and mass produced.

Firstly, improved 3D-printing methods for silicone need to be developed as the method used in this study is inefficient and prone to defects in printed parts. The first issue with the current DIW method is the preparation of silicone material before printing is time consuming and the printer setup has to be repeated every time the nozzle head is removed or the tubing needed to be replaced. Aside from this, when the infill percentage gets lower, the rate of defects increases dramatically, as the silicone will sometime get pulled along the nozzle and not deposit properly.

Futher study into the long-term durability of 3D-printed silicones need to be studied to better understand how 3D-printed silicones react under long term loading, cyclical stresses, and and different environments. Without an accurate understanding of its durability, users will not feel comfortable purchasing a product using 3D-printed silicones compared to conventional materials.

Lastly, based on tactile response, some infill patterns seem to have more desirable stress-strain relationships when compressed in different directions and axis. For instance, the grid pattern has very different tactile response when compressed diagonally to the direction of the internal pattern walls. This response is very different compared to the tactile response when compressed in the direction of printing. Further study can be conducted into the different directionality of some of the infill patterns and how it affects the compressive characteristics.

REFERENCES

Al'aref, S.J., Bobak Mosadegh, Dunham, S. and Min, J.K. (2018). *3D printing applications in cardiovascular medicine*. London, United Kingdom: Elsevier/Academic Press.

Beloshenko, V. *et al.* (2021) 'Mechanical properties of flexible TPU-based 3D printed lattice structures: Role of lattice cut direction and architecture', *Polymers*, 13(17), p. 2986. doi:10.3390/polym13172986.

Boresi, A.P. and Schmidt, R.J. (2003) *Advanced Mechanics of Materials*. 6th edn. New York City, New York: John Wiley & Sons.

Buddhima Rupasinghe (2023). Recycling Silicone-Based Materials: An Overview of Methods. *IntechOpen eBooks*. doi:https://doi.org/10.5772/intechopen.108051.

de la Rosa, S. *et al.* (2024) 'Design and characterization of 3D-printed TPU-based lattice structures. application to methodology for the design of personalized therapeutic products', *Rapid Prototyping Journal*, 30(11), pp. 72–86. doi:10.1108/rpj-08-2023-0287.

Donnelly, B. (2020) *Designing structural components? don't forget about buckling. - engineers rule*, *Engineers Rule*. Available at: https://www.engineersrule.com/designing-structural-components-dont-forget-about-buckling/ (Accessed: 02 May 2026).

Ebe, K. and Griffin, M.J. (2001) 'Factors affecting static seat Cushion Comfort', *Ergonomics*, 44(10), pp. 901–921. doi:10.1080/00140130110064685.

Farid Bensebaa (2013). Nanoparticle Assembling and System Integration. *Interface Science and Technology*, 19, pp.185–277. doi:https://doi.org/10.1016/b978-0-12-369550-5.00004-5.

Fitzsimons, B. and Parry, T. (2009). *Marine Fouling - Fouling of Ships - BEVALDIA*. [online] BEVALDIA. Available at: https://bevaldia.com/marine-fouling/ [Accessed 19 Sep. 2025].

Friedrich, L.M. and Woodcock, J.W. (2025). Inducing inter-filament fusion during embedded 3D printing of silicones. *Additive Manufacturing*, 102, p.104741. doi:https://doi.org/10.1016/j.addma.2025.104741.

Gent, A.N. and Thomas, A.G. (1959) 'The Deformation of Foamed Elastic Materials', *Journal of Applied Polymer Science*, 1(1), pp. 107–113. doi:10.1002/app.1959.070010117.

Hurlbutt, K.M. (2024). *Silicone Resins for Vat Polymerization Printing*. [online] *U.S. Department of Energy Office of Scientific and Technical Information*. United States: U.S. Department of Energy Office of Scientific and Technical Information. Available at: https://www.osti.gov/biblio/2318929 [Accessed 18 Sep. 2025].

Lagerström, M., Wrange, A.-L., Oliveira, D.R., Granhag, L., Larsson, A.I. and Ytreberg, E. (2022). Are silicone foul-release coatings a viable and environmentally sustainable alternative to biocidal antifouling coatings in the Baltic Sea region? *Marine Pollution Bulletin*, [online] 184, p.114102. doi:https://doi.org/10.1016/j.marpolbul.2022.114102.

Liu, D.-S. *et al.* (2016) 'Compressive mechanical property analysis of EVA foam: Its buffering effects at different impact velocities', *Journal of Mechanics*, 33(4), pp. 435–441. doi:10.1017/jmech.2016.98.

McCoul, D., Rosset, S., Schlatter, S. and Shea, H. (2017). Inkjet 3D printing of UV and thermal cure silicone elastomers for dielectric elastomer actuators. *Smart Materials and Structures*, 26(12), p.125022. doi:https://doi.org/10.1088/1361-665x/aa9695.

Moon, J. *et al.* (2020) 'Recycling of bio-polyurethane foam using high power ultrasound', *Polymer*, 186, p. 122072. doi:10.1016/j.polymer.2019.122072.

Naoum, K. de and Piccoli, R. (2022). *Infill in 3D Printing: Definition, Main Parts, and Different Types*. [online] www.xometry.com. Available at: https://www.xometry.com/resources/3d-printing/what-is-infill-in-3d-printing/ [Accessed 19 Sep. 2025].

Ottenbrite, R.M. and Javan, R. (2005). Biological Structures. *Encyclopedia of Condensed Matter Physics*, pp.99–108. doi:https://doi.org/10.1016/b0-12-369401-9/00698-7.

Ree, I. and Kim, J.H. (2026) 'Citric acid-engineered cellulose as a high-performance bio-filler for polyurethane foams: Simultaneous enhancement of acoustic absorption and cushioning properties', *Journal of Environmental Chemical Engineering*, 14(2), p. 122167. doi:10.1016/j.jece.2026.122167.

Rodriguez, N. *et al.* (2021) '3D printing of high viscosity reinforced silicone elastomers', *Polymers*, 13(14), p. 2239. doi:10.3390/polym13142239.

Ryszczuk, H. *et al.* (2026) 'Soft solutions for complex problems: 3D-printed silicone in healthcare', *Biomaterials Advances*, 185, p. 214870. doi:10.1016/j.bioadv.2026.214870.

Sharma, P., Dhanopia, A.K. and Joshi, D. (2020). An experimental study on carbon fiber thickness and layer thickness of depositing material in fused deposition modeling. *Materials Today: Proceedings*, 44(6). doi:https://doi.org/10.1016/j.matpr.2020.10.722.

Silva, P. *et al.* (2024) 'Static factors in sitting comfort: Seat foam properties, temperature, and contact pressure', *Applied Sciences*, 14(17), p. 7753. doi:10.3390/app14177753.

Śliwiak, M., Bui, R., Brook, M.A. and P. Ravi Selvaganapathy (2021). 3D printing of highly reactive silicones using inkjet type droplet ejection and free space droplet merging and reaction. *Additive manufacturing*, 46, pp.102099–102099. doi:https://doi.org/10.1016/j.addma.2021.102099.

Truby, R.L., Wehner, M., Grosskopf, A.K., Vogt, D.M., Uzel, S.G.M., Wood, R.J. and Lewis, J.A. (2018). Soft Somatosensitive Actuators via Embedded 3D Printing. *Advanced Materials*, 30(15), p.1706383. doi:https://doi.org/10.1002/adma.201706383.

Wolf, A.T. and Stammer, A. (2024). Chemical Recycling of Silicones—Current State of Play (Building and Construction Focus). *Polymers*, [online] 16(15), pp.2220–2220. doi:https://doi.org/10.3390/polym16152220.

Wong, L.Y., Ganguly, S. and Tang, X. (Shirley) (2024). 3D vat photopolymerization printing of hydrophilic silicone-based microfluidic devices and the effect of cellulose nanocrystals as additives for improved printing accuracy. *Additive Manufacturing*, 86, p.104177. doi:https://doi.org/10.1016/j.addma.2024.104177.

Zhao, T., Yu, R., Li, S., Li, X., Zhang, Y., Yang, X., Zhao, X., Wang, C., Liu, Z., Dou, R. and Huang, W. (2019). Superstretchable and Processable Silicone Elastomers by Digital Light Processing 3D Printing. *ACS Applied Materials & Interfaces*, 11(15), pp.14391–14398. doi:https://doi.org/10.1021/acsami.9b03156.

Zhou, L., Gao, Q., Fu, J., Chen, Q., Zhu, J., Sun, Y. and He, Y. (2019). Multimaterial 3D Printing of Highly Stretchable Silicone Elastomers. *ACS Applied Materials & Interfaces*, 11(26), pp.23573–23583. doi:https://doi.org/10.1021/acsami.9b04873.

Zhang, L. *et al.* (2018) 'Energy absorption characteristics of metallic triply periodic minimal surface sheet structures under compressive loading', *Additive Manufacturing*, 23, pp. 505–515. doi:10.1016/j.addma.2018.08.007.

APPENDIX

Appendix A: Open Access to Image Rights

Compressive Mechanical Property Analysis of Eva Foam: Its Buffering Effects at Different Impact Velocities

Author: Liu, D.-S.; Chen, Z.-H.
Publication: Journal of Mechanics
Publisher: Oxford University Press
Date: 2016-09-22

Copyright © 2016, © The Society of Theoretical and Applied Mechanics 2016

Order Completed

Thank you for your order.

This Agreement between Elijah Lim Rong Yao ("You") and Oxford University Press ("Oxford University Press") consists of your license details and the terms and conditions provided by Oxford University Press and Copyright Clearance Center.

Your confirmation email will contain your order number for future reference.

License Number 6271431219209 — Printable Details

License date May 17, 2026

Licensed Content

Licensed Content Publisher	Oxford University Press
Licensed Content Publication	Journal of Mechanics
Licensed Content Title	Compressive Mechanical Property Analysis of Eva Foam: Its Buffering Effects at Different Impact Velocities
Licensed Content Author	Liu, D.-S.; Chen, Z.-H.
Licensed Content Date	Sep 22, 2016
Licensed Content Volume	33
Licensed Content Issue	4

Order Details

Type of Use	Thesis/Dissertation
Requestor type	Educational Institution/Non-commercial/ Not for-profit
Format	Electronic
Portion	Figure/table
Number of figures/tables	1
Will you be translating?	No

About Your Work

Title of new work	STUDY OF MECHANICAL PROPERTIES OF 3D-PRINTED SILICONE FOR CUSHIONING APPLICATIONS
Institution name	Universiti Tunku Abdul Rahman
Expected presentation date	May 2026

Additional Data

Portions	Figure 4
The Requesting Person / Organization to Appear on the License	Elijah Lim Rong Yao

Figure C-1: Reprinted with Permission from Copyright 2016 Oxford University Press to Reuse Stress Strain Curve of EVA Foam (Liu et al., 2016) Image in Figure 4.5.

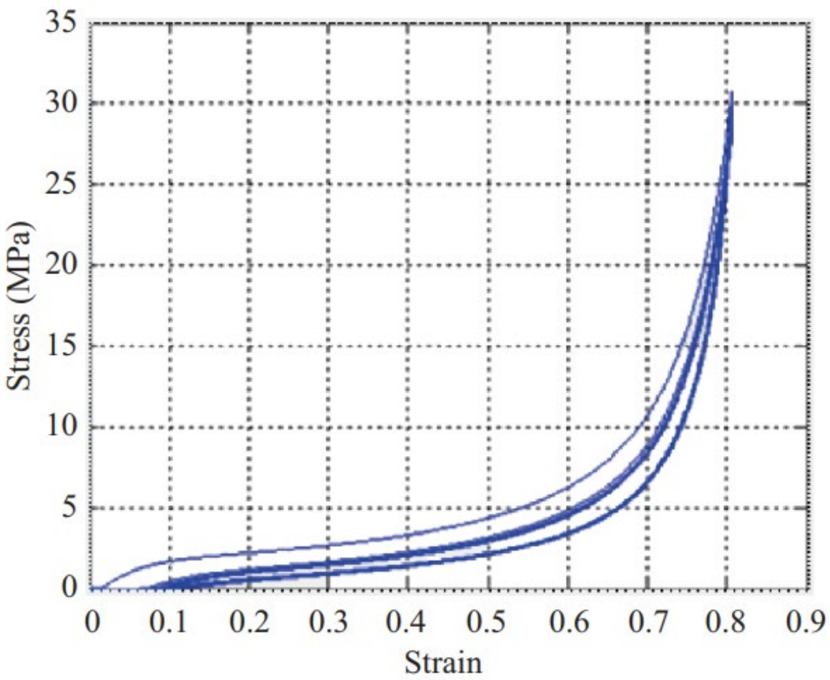

Figure 4.1: Stress Strain Curve of EVA Foam. (Liu et al., 2016) Reprinted with Permission from Copyright 2016 Oxford University Press